IRANIAN JOURNAL OF PHYSICS RESEARCH

Iranian Journal of Physics Research, Vol. 11, No. 3, 2011

Construction and testing of a hydrogen cracking cell

F Sahra Gard

Department of Physics, Sultan Qaboos University, P.O.Box: 36 Al-Khode 123 Muscat, Sultanate of Oman
E-mail: gard@squ.edu.om

(Received 1 May 2010 , in final from 24 May 2011)

Abstract

A UHV atomic hydrogen-cracking cell has been constructed to produce atomic hydrogen in order to perform *in-situ* cleaning of semiconductor samples. The cell was calibrated and tested with the objective of cleaning the III-V semiconductor samples such as GaAs. Mass spectroscopy studies during the atomic hydrogen cleaning of the GaAs samples revealed the chemical process of the hydrogen cleaning. X-ray Photoemission Spectroscopy (XPS) was also carried out on the samples at different stages of cleaning. Desorption of the native oxide from GaAs samples resulted in a smooth surface, which was confirmed by Reflection High Energy Electron Diffraction (RHEED).

Keywords: DNA, semicondoctors, GaAs, MBE, XPS, RHEED

1. Introduction

Ex-situ chemical degreasing and etching followed by *in-situ* cleaning of semiconductors surfaces is essential to obtain a well-ordered surface with minor amount of contamination before growth of thin films. *Ex-situ* chemical etching method by itself is not ideal, usually one element of most binary III-V semiconductors such as GaAs tends to be preferentially etched. *In-situ* cleaning methods such as annealing, crystal cleavage, ion bombardment and atomic hydrogen cleaning under UHV environment are the most commonly used to produce clean surfaces. Depending on the type of the semiconductors and their crystallographic directions, there are some limitations to the above mentioned techniques. For example, crystal cleavage along [110] is a useful technique for substrate preparation of zincblende structure III-V semiconductors. However, the reproducibility is not always guaranted. There can be difficulties in *in-situ* cleaving and handling the samples of other crystallographic directions. For example, it is not possible at all to cleave polar [111] and [100] surfaces in order to produce a smooth clean surface.

1.1. Thermal cleaning

Thermal cleaning process will remove the native contaminations such as carbon and oxygen from a surface by annealing the samples at relatively high temperature. This method is the most preferred technique to produce a clean metallic or semiconductor samples. In the case of III-V semiconductor materials, thermal cleaning is not an ideal approach due to non-congruent sublimation. Both III and V group elements will sublime and will be adsorbed as a result of thermal cleaning treatment. Below the congruent sublimation temperature T_{cs}, the partial equilibrium pressure of group III elements, and hence the sublimation rate, are higher than that for the group V elements. Therefore, at elevated temperatures below T_{cs}, there will be an excess of the group V elements on the surface. However, the group V elements tend to form molecular dimmers (V_2) which are thermodynamically more stable than the usual molecular species (V_4). Then, dimmers recombine to form tetramers with higher partial pressures and they themselves sublime, which leads to the so-called congruent sublimation. On the other hand, above T_{cs}, the desorption rate of group V atoms is higher, producing a net surface excess of group III atoms on the sample. Even if the temperatures required to desorb contaminations are below the melting point for the III-V compound, they may result in non-congruent sublimation, altering and if not effectively destroying the surface of the sample. The congruent sublimation temperature of some common III-V semiconductor materials is listed in Table 1.

1.2. Ion bombardment

During the ion bombardment cleaning method, a beam of energetic ions such as 0.5-5 keV Ar^+ is incident on the sample surface. These ions usually have a large screened Columbic interaction cross section with the atoms on the

Table 1. Congruent sublimation temperatures for some common III-V semiconductor materials [1].

Compound	GaAs	GaP	GaSb	InAs
($T_{cs}\pm 5$) [K]	868	853	728	660

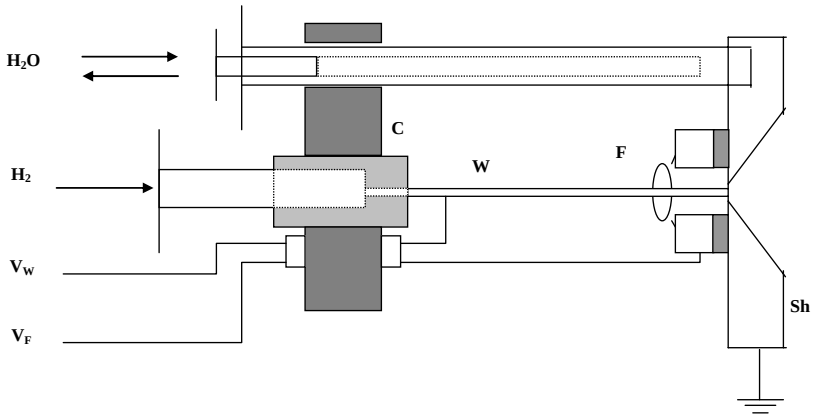

Figure 1. Schematic diagram of the H-cracking cell.

surface, which can cause cascade collisions through the neighboring atoms. Depending on the energy of incident atoms and the type of the substrate, these cascade collisions may result in a high density of defects and a major rearrangement of the crystal structure, the so - called amorphization. For low energetic ions, the collision cascade happens on the surface. The top layer of surface and adsorbate atoms are ejected in a process called sputtering. The sputtering itself causes significant damage to both surface and sub surface, and hence ion bombardment is normally followed by annealing. During annealing, defects such as dislocation tend to migrate to the surface where they combine and dissipate, tending to restore the physical order of the sample. Unfortunately, the annealing process also leads to some extensive preferential surface segregation of bulk impurities and implanted incident ions, which should be removed by further cycles of bombardment and annealing. Generally, several cycles of ion bombardment and annealing are required to prepare a relatively clean and damage-free surface. However, there are other effects, which must be considered, such as preferential sputtering and non-congruent sublimation of group V species from the surface during the annealing of the sample. The surface topography, even after cyclic Ion Bombardment and annealing, may also exhibit undesired features on the submicron scale such as rippling, droplets and columnar features known as cones, formed during recrystallization of the amorphous surface region.

2. Construction of hydrogen cleaning (AHC)

Historically, the physical principle of the first type of the atomic hydrogen (H*) sources was based on production of hydrogen atoms in a plasma created by electron cyclotron resonance (ECR). The early studies showed that desorption of oxides and hydrocarbons, two of the most persistent semiconductor surface contaminants, may occur at a lower temperature than the ones required by only annealing in vacuum[2 - 4]. However, ECR sources are expensive and most critically produce ionized and energetic particles, which cause sputter damage to the substrate. Nowadays, the commercial available hydrogen cracking sources are based on two different principles and designs. The first types of the cells consist of a hot tungsten filament placed in a relatively wide tube with the chamber backfilled with hydrogen. In this design, only a small fraction of the hydrogen molecules hits the hot filament and dissociates in hydrogen atoms. The dissociation efficiency with this method is relatively low. For example, in the "Atom-H" source from EPI Europe, UK, molecular hydrogen are cracked on a hot (1800°C) tungsten filament, which is coaxial with the water cooled inlet tube. The overall efficiency of the cracking of H_2 to H*, is estimated to be 3%, using a platinum calorimeter in front of the source to detect the recombination rate of 2H to H_2 [5,6]. Although a cracking efficiency of 6-7% could be achieved by increasing the filament temperature to 2100°C, [5,6] the vapor pressure of tungsten is ~10^{-9} mbar at this temperature, which may cause additional contamination of the sample [7]. Additional problem with this type of hydrogen sources is the undesirable heat load produced in the UHV chamber, and consequently the degassing of the source itself and the chamber walls in the vicinity to the source. In the second types of hydrogen cracking cells, the molecular hydrogen is cracked as it passes through a tungsten capillary heated by electron bombardment, extracted from one or two tungsten filament/s. This design of atomic hydrogen source is known as the Bertel type [8,9] and has several advantages over the other types of sources. For example, the cracking efficiency is much higher, as a result of the high collision rate of H_2 molecules with the capillary's wall. The hydrogen cracking efficiency is reported to be up to 100% [10]. The hydrogen-cracking cell, which is built in our lab at a fraction of the cost of commercial one, is a rather simplified copy of the Bertel type hydrogen cracking cell. The schematic illustration of the cell is shown in figure 1. The tungsten capillary (W) is connected to a stainless tube via an insulating ceramic adapter (C). The capillary

Table 2. Capillary's physical dimension.

Length [mm]	Inner diameter [mm]	Outer diameter [mm]
50	0.6	1.6

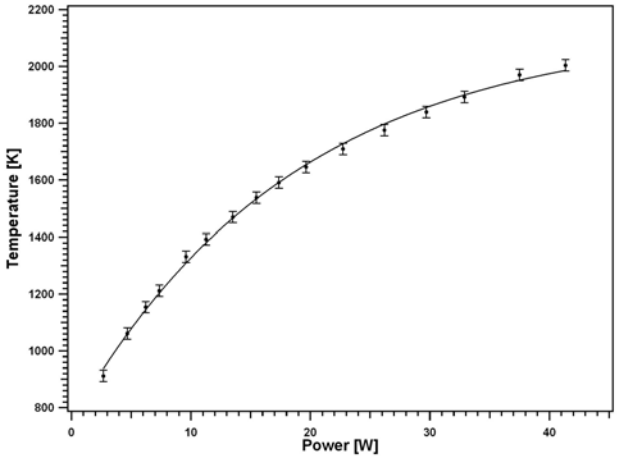

Figure 2. Capillary temperature as a function of the applied power to the H-cracking cell.

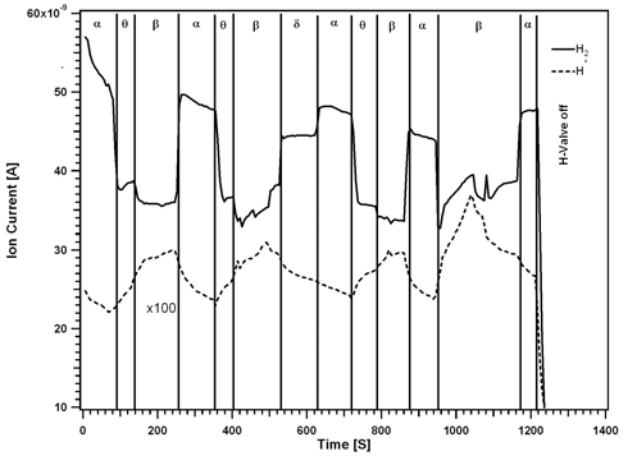

Figure 3. H_2 signal (solid line) and H signal (dashed line) from the quadrupole mass spectrometer.

dimensions are given below in table 2. The capillaries were purchased from the Plansee Company, Austria.

Pure hydrogen (99:99%) molecules can be admitted into the capillary through the stainless tube via a leak valve. A tungsten wire (F) is installed around the outlet of the capillary, which acts as a filament. A water-cooled copper shield with a pinhole (Sh) is mounted in front of the capillary to protect the substrate from the heat, produced by the hydrogen cell. The copper shield can also act as an aperture to collimate the atomic hydrogen beam. A maximum potential difference of V_W = 1000 V, between the filament and capillary, may be applied to produce an emission current of 40 mA, which is the usual operating temperature of the hydrogen cell. Capillary temperature as a function of the electrical power is shown in figure 2. The temperature was measured by a Pyrometer.

2.1. Dissociation degree of the hydrogen cracking cell

A comprehensive theoretical and experimental study of the dissociation degree of the Bertel type hydrogen-cracking cell is reported elsewhere [9]. In the current study, a mass spectroscopic measurement was performed in order to measure the dissociation degree of the hydrogen-cracking cell. A quadrupole mass spectrometer (QMS) was placed in front of the H-cell in the preparation chamber. The distance between the mass spectrometer head and the aperture of the H-cell (water-cooling shield), was about 150mm. Figure 3 shows the hydrogen molecules (solid line) and the hydrogen atoms (dashed line) signals of the QMS. The atomic hydrogen signal is multiplied by 100 in order to make comparison between the H_2 molecules and H atoms signals easier.

The graph is divided into different regions: α, where the H-cell is off, γ, θ, and β, where the H-cell operats at 30W, 40W and 60W electrical power, respectively. The H_2 molecule level decreases upon increasing the electrical power applied to the hydrogen cell, and the atomic hydrogen level increases by increasing the power. High reactivity of the hydrogen atoms makes them very difficult to be detected by the mass spectrometer. However, a tendency of increasing the atomic hydrogen level is evident when the hydrogen cell is operated at high electrical power. Clearly, a drop of ~30% of H_2 signal is due to convolution of the change of the capillary's conductance because of the heat and the dissociation of H_2 molecules.

2. 2. Physical principle of AHC

Several studies have demonstrated that hydrogen atoms are very efficient "catalysts" for cleaning the III-V semiconductors, including GaAs at low substrate temperature [11 , 12]. However, a few studies explored the surface reaction mechanism underlying the hydrogen cleaning process. Auger Electron Spectroscopy (AES) studies from a GaAs substrate, in the presence of hydrogen atoms, have shown that carbon is removed at a temperature of 200°C and all oxygen is removed at a temperature of 400°C [13]. Mass spectroscopic measurements of the hydrogen cleaning mechanism of the GaAs substrate suggest that arsenic molecules (As_2 or $1/2As_4$) will be liberated upon the reaction of As oxides with hydrogen atoms[14]. The chemical reactions, which have been suggested for the liberation of arsenic molecules, are given below:

$$As_2O_x + 2_xH \rightarrow H_2O\uparrow + As_2,$$

Or

$$As_2O_x + 2_xH \rightarrow H_2O\uparrow + 1/2As_4,$$

where x = 1, 2 or 5 represents the various oxides of arsenic. The removal of the Ga_2O_3 is believed to proceed through the formation and removal of volatile Ga_2O, as expressed in the following chemical reaction[15]:

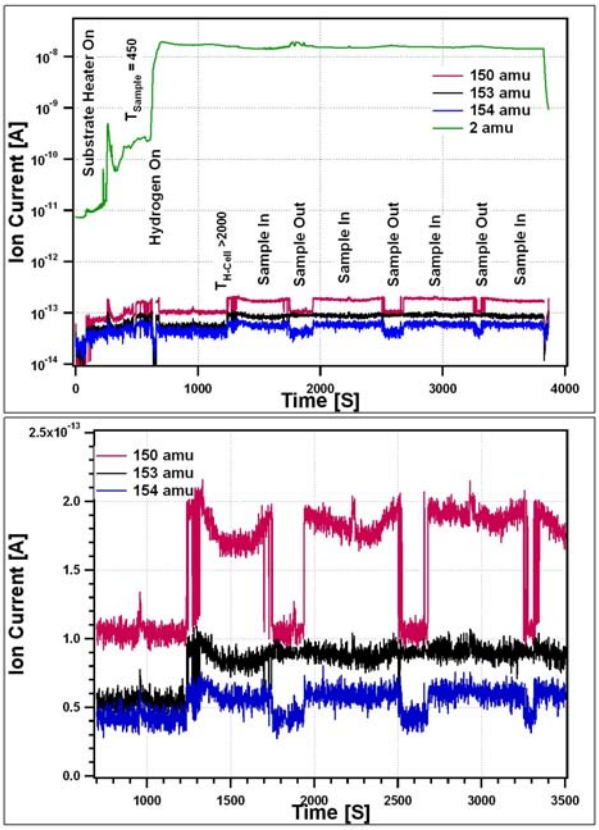

Figure 4. Quadrupole mass spectrometry of the GaAs substrate during H-cleaning of the GaAs substrate (A). Mass spectra of 150 u, 153 u, 154 u are shown on a larger scale in (B).

$$Ga_2O_3 + 4H \rightarrow 2H_2O\uparrow + Ga_2O.$$

In the current study, a GaAs substrate at 450°C was exposed to atomic hydrogen in the UHV chamber. The operating hydrogen pressure was about 1×10^{-6} Torr. A QMS was installed in UHV chamber facing the GaAs sample in order to monitor the desorbed species from the surface. The GaAs sample was cleaved from commercially available GaAs (100) wafer. The substrate was degreased in 20 ml trichlorethylene for 2 minutes, then in 20 ml acetone for 1 minute and finally in 10 ml methanol for 2 minutes, using a ultrasonic bath. It was then rinsed with deionized water before being etched in concentrated H_2SO_4 for 30 seconds to remove the excess water from the substrate. The substrate was finally etched for 90 seconds in 20ml of stagnant $H_2SO_4/H_2O/H_2O_2$ (6:1:1) volume ratio solution, while rapidly stirring to avoid selective etching or bubble formation on the substrates. The etch rate is estimated to be about 1.5 m/min. It was then rinsed with deionized water and blow-dried using dry nitrogen gas before mounting it on a substrate holder using indium soldering. The mass spectrometer was tuned to monitor As_2 or $1/2As_4$ with atomic mass unit of 150 *u*, and Ga_2O with 154 *u*. An additional ion mass signal of 153 *u* was also monitored simultaneously as a measure of background species present in the chamber, since it cannot be related to any conceivable Ga- or As- related ions from the substrate. Figure 4(A) shows the change of mass signals of the detected ions during the H-cleaning. Figure 4(B) shows part of the same spectra for masses 150 *u*, 153 *u* and 154 *u*, on a larger scale. Desorption of Ga_2O and As_2 was observed while the sample was brought in line to the atomic hydrogen beam, in front of the QMS, as indicated by "sample in" in figure 4(A). The liberation of Ga_2O and As_2 did not take place when the sample was kept away from the atomic hydrogen beam, as indicated by "sample out" in figure 4(A). Signal intensity of mass 153 *u* was increased when the H-cel temperature was set to 2000 K. Otherwise, it did not change throughout the whole experiment. This indicates that the observed mass of 153 *u* signal does not receive any contribution from the sample, while signal intensities of the masses 150 amu and 154 amu receive contribution from the GaAs substrate. This is a direct observation of the liberation of As_2 or 1/2 As_4 and Ga_2O from the GaAs sample.

2. 3. XPS analysis

Next, in another experiment, the X-ray Photoemission Spectroscopy (XPS) was used on a GaAs (100) sample at different stages of hydrogen cleaning. The XPS studies were carried out in an OMICRON Multiprobe System at a base pressure of better than $1x10^{-10}$ Torr with a monochromatic Al source 1486 eV. The sample surface was kept normal to the axis of the analyzer input lens. The source was operated at an emission current of 20 mA and an anode voltage of 15 kV. The analyzer pass energy was set at 50 eV and the step size was set at 0.5 eV for long range energy scan. For short range scan, the analyzer pass energy and step size was set at 18 eV and 0.05 eV, respectively. Under these conditions, the measured full width at half maximum (FWHM) of the Ag $3d_{5/2}$ line is 0.8 eV and this is a measure of the energy resolution of the instrument for these measurements.

Photoelectron peaks were recorded and resolved by spectrum synthesis in which the spectral line shapes were fitted by mixed Gaussian-Lorentian combinations. Relative atomic concentrations of the species on the surface were calculated from the intensities of the major photoelectron spectral lines (integrated peak areas) after subtracting a linear background.

During the cleaning of the samples, pure molecular hydrogen %99:99 was introduced directly to the H-cracker cell. The hydrogen doses are measured here in terms of molecular hydrogen exposures dose in kilo Longmuir (KL), ($1KL=10^{-6}$Torr.s). During AHC, the chamber pressure was around $1x10^{-10}$ Torr, with typical dose times of 25-50 minutes, corresponding to H_2 doses of 15-30 KL. GaAs sample was degreased and chemically etched prior to introduction to UHV chamber (see section 2.2). The sample temperature was set to be (450±25)° C, which was measured by a pyrometer.

Figure 5 shows a large energy scan of the GaAs sample at different stages of hydrogen cleaning; as received, without any hydrogen treatment (A), after 15 KL hydrogen exposure (B) and after 30 KL hydrogen

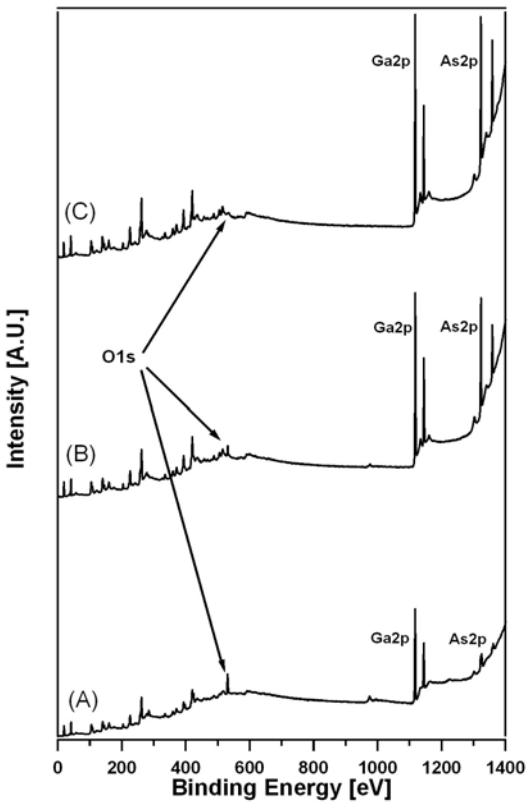

Figure 5. The large range energy scan of a GaAs sample at different stages of hydrogen cleaning; as received (A), after exposure 15 KL atomic hydrogen (B) and 30 KL atomic hydrogen (C).

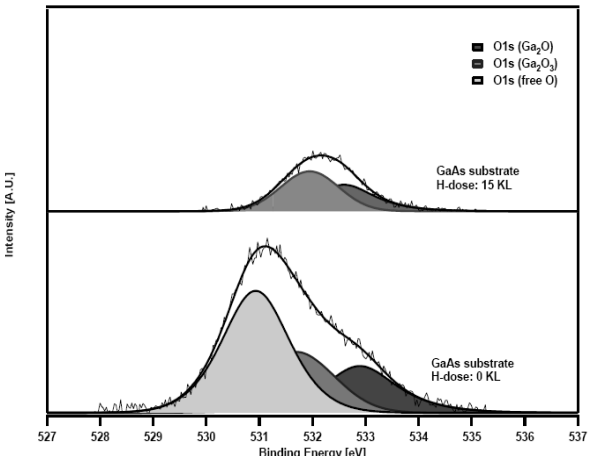

Figure 6. High resolution XPS scan of the O1s peak as received (bottom) and after 15KL hydrogen exposure (top).

exposure (C). The intensity of $Ga2p_{1/2}$ at 1144 eV, $Ga2p_{3/2}$ at 1117 eV, As $2p_{1/2}$, at 1359 eV and As $2p_{3/2}$ at 1323 eV are progressively increased by increasing the atomic hydrogen dose. The position of O1s peak at 531 eV is indicated on the spectra. It disappears by increasing the exposure of the sample to the atomic hydrogen.

High resolution XPS scan of the O1s peak is shown in figure 6. It reveals the existence of free oxygen at binding energy (531.0±0.2)eV and oxygen in form of Ga oxides: Ga_2O_3 at (531.8±0.2)eV and Ga_2O at (532.8±0.2)eV on the surface of as-received sample (without atomic hydrogen treatment). The free oxygen component disappears after 15 KL hydrogen exposure of the sample, and the other components of O1s is readily decreased as well. After 30KL hydrogen treatment the sample, no O1s peak was observed. The relative peak's areas of the O1s components are given below in table 3.

Table 3. The relative peak's area of O1s components during different stage of hydrogen cleaning H-dose O.

H-dose	O- (free)	O- (Ga_2O_3)	O-(Ga_2O)
0 KL	0.50	0.28	0.22
15 KL	0.00	0.57	0.43
30 KL	0.00	0.00	0.00

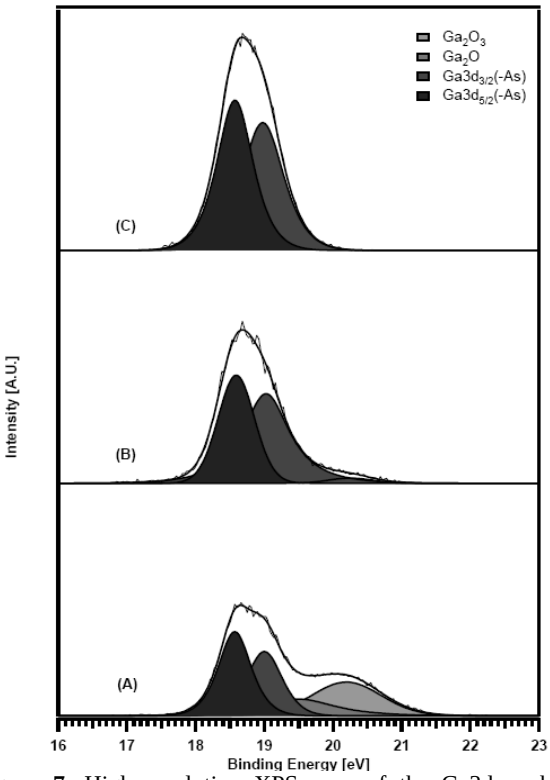

Figure 7. High resolution XPS scan of the Ga3d peak as received (A), after 15 KL hydrogen exposure (B) and after 30 KL hydrogen exposure (C).

The Ga3d spectra of the GaAs sample at different stages of the hydrogen cleaning is shown in figure 7. Prior to hydrogen cleaning (A), the spectrum contains 4 major components with binding energies of (18.6±0.2) eV, (19.0±0.2) eV, (19.5±0.2) eV and (20.2±0.2) eV corresponding to $Ga3d_{5/2}$ (-As), $Ga3d_{3/2}$ (-As), Ga_2O, and Ga_2O_3, respectively.

After 15 KL hydrogen treatment of the sample, the Ga_2O component disappears and small residue of Ga oxide in form of Ga_2O_3 is observed on the surface (see figure 7(B)). Further hydrogen treatment of the GaAs sample removed all the Ga oxides from the surface, as shown in figure 7(C). The relative peak's areas of the Ga3d components are given below in table 4.

Table 4. The relative peak's area of Ga3d components during different stages of hydrogen cleaning.

H-dose	$Ga3d_{5/2}$ (-As)	$Ga3d_{3/2}$ (-As)	Ga-(Ga_2O)	Ga-(Ga_2O_3)
0 KL	0.33	0.26	0.15	0.26
15 KL	0.54	0.43	0.00	0.03
30 KL	0.59	0.41	0.00	0.00

Table 5. The relative peak's area of $Ga2p_{3/2}$ components during different stages of hydrogen cleaning.

H-dose	$Ga2p3_{/2}$ (-As)	Ga-(Ga_2O)	Ga-(Ga_2O_3)
0 KL	0.19	0.60	0.21
15 KL	0.57	0.38	0.05
30 KL	1.00	0.00	0.00

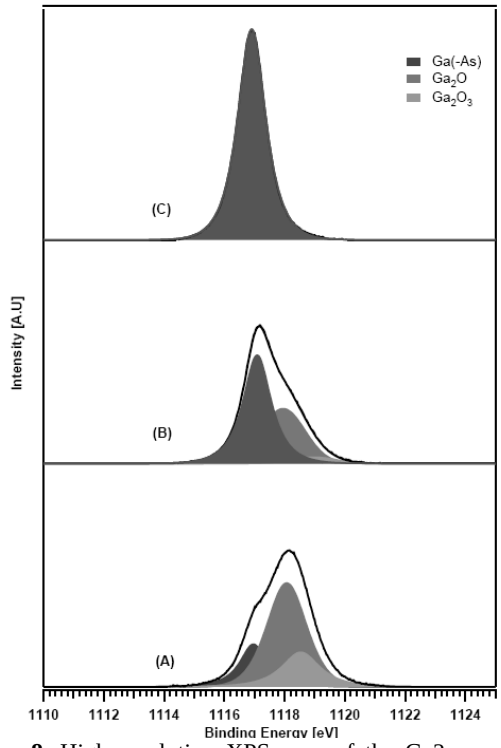

Figure 8. High resolution XPS scan of the $Ga2p_{3/2}$ peak as received (A), after 15KL hydrogen exposure (B) and after 30 KL hydrogen exposure (C).

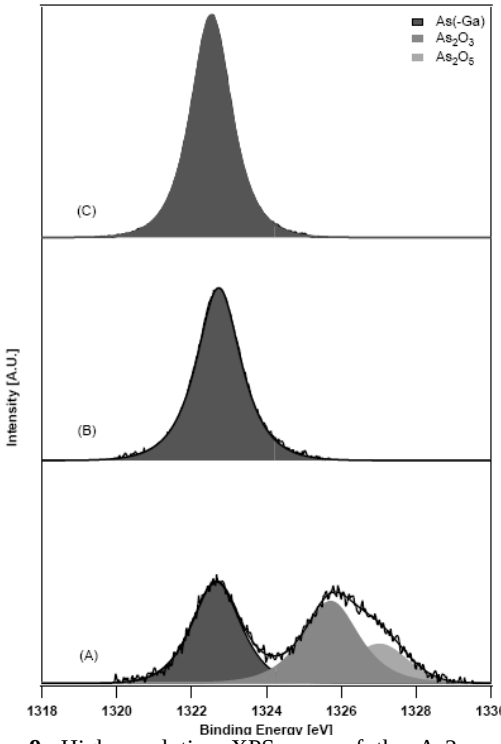

Figure 9. High resolution XPS scan of the As2p peak as received (A), after 15KL hydrogen exposure (B) and after 30 KL hydrogen exposure (C).

Figure 8 shows a high resolution of $Ga2p_{3/2}$ line during the process of hydrogen cleaning of the sample. The $Ga2p_{3/2}$ and G $2p_{1/2}$ lines, in comparison to Ga3d line, represent smaller sampling depths and hence are more sensitive to surface modification. In addition, the identification and quantification of the components of Ga using the $2p_{3/2}$ and $Ga2p_{1/2}$ lines, would be statistically more accurate than using 3d region due firstly to their simple line shapes, which consist of only a single photoelectron line. Secondly, the $Ga2p_{3/2}$ and $Ga2p_{1/2}$ peaks have the highest intensities in XPS spectra of GaAs (see figure 5).

The corresponding binding energies of the $Ga2p_{3/2}$ at (1117.0±0.2) eV, Ga_2O at (1118.0±0.2) eV and Ga_2O_3 at (1118.8±0.2) eV lines were observed on the surface of untreated GaAs sample (see figure 8(A)). The Ga oxide components were decreased and the $Ga2p_{3/2}$ line intensity increased after 15 KL hydrogen treatment (see figure 8(B)). All Ga oxide components disappeared by further hydrogen treatment (see figure 8(C)). The relative peak's areas of the $Ga2p_{3/2}$ components are given below in table 5.

The As 3d spectrum of the untreated GaAs sample consisted of three components at (41.0±0.2), (44.0±0.2) and (45.2±0.2) eV, corresponding to As(-Ga), As_2O_3, and As_2O_5, respectively. The $As2p_{3/2}$ peaks were found at energies of (1322.7±0.2), (1325.9±0.2) and (1326.9±0.2) eV. Since the As2p lines are more surface sensitive than As 3d lines, only the $As2p_{3/2}$ spectra are included here (see figure 9). The relative peak's area of $As2p_{3/2}$ components, during different stages of hydrogen cleaning, are given in table 6.

The As oxides were progressively decreased by exposure of the sample to atomic hydrogen flux. It is seen in figure 9 (B) that almost all the As oxides are removed from the sample after only 15 KL hydrogen exposure of the sample. The intensity of $As2p_{3/2}$ line of As(-Ga) was increased by further hydrogen treatment of

Table 6. The relative peak's area of As2p $_{3/2}$ components during different stages of hydrogen cleaning.

H-dose	$As2p_{3/2}$ (-Ga)	As-(As_2O_3)	As-(As_2O_5)
0 KL	0.43	0.40	0.17
15 KL	1.00	0.00	0.00
30 KL	1.00	0.00	0.00

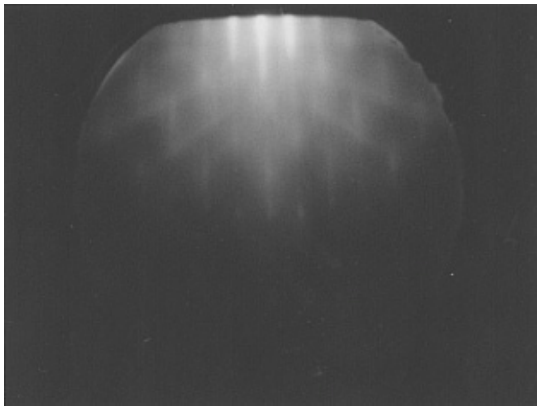

Figure 10. RHEED pattern of a GaAs substrate cleaned by dosing to 30 KL hydrogen flux at 450° C substrate temperature.

the sample to 30 KL hydrogen exposure.

Reflection high energy electron diffraction (RHEED) was also used to assess the quality of the GaAs surface. Figure 10 illustrates the RHEED pattern of GaAs substrate along (110) direction. The sample has been exposed to 30 KL hydrogen. The streaky (4x3) RHEED pattern indicates a smooth surface.

3. Conclusion

An atomic hydrogen-cracking cell has successfully been constructed at a fraction of the commercial available systems. The cell was calibrated and tested to clean semiconductor samples. Mass spectroscopy studies of the GaAs samples, during the atomic hydrogen cleaning, revealed the chemical process of the hydrogen cleaning. High resolution X-ray Photoemission Spectroscopy (XPS) was also carried out on a GaAs sample at different stages of hydrogen cleaning. XPS studies confirmed desorption of the native oxide from GaAs sample, which resulted in a smooth surface. The Reflection High Energy Electron Diffraction (RHEED) pattern confirmed a clean and smooth GaAs surface.

References

1. C E C Wood, K Singer, T Ohashi, L R Dawson and A J Noreika, *J. Appl. Phys.* **54** (1983) 2732.
2. N Kondo and Y Nanishi, *Jpn. J. Appl. Phys.* **28** (1989) L7.
3. J F Klem J Y Tsao, J L Reno, A Dayte and S Chadda, *J. Vac. Sci. Technol. A* **9** (1991) 2996.
4. I Suemune, Y Kunitsugu, Y Kan and M Yamanishi *Appl. Phys. Lett.* **55** (1989) 760.
5. EPI Application Note No. 1-96; A Sutoh, Y. Okada and M Kawabe, *Jpn. J. Appl. Phys*. **34**, 2 (1995) L 1379.
6. EPI Application Note No.3-98; *MBE Products group*, (1998) Unpublished.
7. A Sotoh, Y Okada, and M Kawabe, *Jpn. J. Appl. Phys.* **2** 34 (1995)L 1379.
8. U Bischle, and E Bertel, *J. Vac. Sci. Technol.* A **11** (1993) 458.
9. C Eibl, G Lackner, and A Winkler, *J. Vac. Sci. Technol.* A **16** (1998) 2979.
10. http://www.oxsci.com.
11. E J Petit, and F Houzay, *J. Vac . Sci. Technol.*, B **12** (1994) 2.
12. A Takamori, and S Sugata, K Asakawa, E Miyauchi and H Hasimoto, *Jap. J. Appl. Phys.*, **26**, 2 (1987) L142.
13. T Sugaya, and M Kawabe, *Jap. J. Appl. Phys.*, **30**, 3A (1991) L402.
14. M Yamada, and Y Ide, *Jap. J. Appl. Phys.*, **33**, 5A (1994) L671.
15. M Yamada, Y Ide, and K Tone, *Jap. J. Appl. Phys.*, **31**, 8B (1992) L1157.